

Monitoring MBE substrate deoxidation via RHEED image-sequence analysis by deep learning

Abdourahman Khaireh-Walieh,¹ Alexandre Arnoult,¹ Sébastien Plissard,¹ and Peter R. Wiecha^{1,*}

¹LAAS-CNRS, Université de Toulouse, CNRS, UPS, F-31400 Toulouse, France

Reflection high-energy electron diffraction (RHEED) is a powerful tool in molecular beam epitaxy (MBE), but RHEED images are often difficult to interpret, requiring experienced operators. We present an approach for automated surveillance of GaAs substrate deoxidation in MBE using deep learning based RHEED image-sequence classification. Our approach consists of a non-supervised auto-encoder (AE) for feature extraction, combined with a supervised convolutional classifier network. We demonstrate that our lightweight network model can accurately identify the exact deoxidation moment. Furthermore we show that the approach is very robust and allows accurate deoxidation detection during months without requiring re-training. The main advantage of the approach is that it can be applied to raw RHEED images without requiring further information such as the rotation angle, temperature, etc.

Keywords: RHEED, deep learning, molecular beam epitaxy, substrate deoxidation

I. INTRODUCTION

Reflection high-energy electron diffraction (RHEED) is a widely used in-situ control method in molecular beam epitaxy (MBE) [1–4]. RHEED diffraction patterns provide information about the crystal surface with atomic resolution and as the ultra high vacuum in typical growth chambers allows an easy integration of electron beam systems in MBEs, RHEED has become a standard in-situ characterization instrument in MBE, enabling unprecedented accuracy in monitoring the crystal growth. RHEED is highly sensitive to several key MBE parameters like the growth rate, the crystal structure, the lattice parameter and strain, etc [5–9]. However, RHEED images can be difficult to interpret since the diffraction patterns produce information in the Fourier-space. Furthermore, the actual recorded patterns are very sensitive to calibration, and often also dynamic variations in the patterns over several time-scales contain valuable information, rendering their analysis even more challenging. Real-time exploitation of RHEED information is therefore often limited to easily accessible information like deposition rate, sophisticated analysis is often a posteriori, on recorded RHEED images or videos. Due to the complexity of the task, RHEED interpretation usually requires experienced operators, possessing years of machine-specific training.

A common application of RHEED is the monitoring of the native oxide removal from commercial substrates prior crystal growth. Surface oxidation of a few nanometers due to exposure to oxygen is unavoidable during transport of epitaxial substrates, which renders their surface non-crystalline. This oxide needs to be removed before any epitaxial material deposition, which is usually done by heating. In the case of gallium arsenide (GaAs), the substrate is slowly heated to around 610°C, while stabilizing the crystal with a constant arsenic flux of around 1.2×10^{-5} Torr, to avoid As evaporation. Once the oxide is removed, in order to avoid damaging of the crystal, further temperature ramping needs to be stopped, usually temperature is in fact decreased. To detect the deoxidation, the MBE operator supervises the RHEED image during tempera-

ture increase, and once the diffraction pattern of a crystalline surface starts to form, the operator manually ends the heating procedure. Not only is the constant presence of the operator required, due to its manual character the deoxidation procedure is furthermore error-prone. Automatic detection of the deoxidation is challenging, first because RHEED patterns are often weak since the raw substrate surfaces are not atomically flat, and second because the RHEED image contrast is dependent on some parameters like filament current or electron beam angle, and hence is not exactly constant in each run. Finally, the substrate is usually laying on a rotating sample holder, hence the RHEED pattern constantly changes.

Methods from artificial intelligence including deep learning are increasingly applied to nano- and material-science [10–14]. Recently, first attempts have been reported to use statistical methods and machine learning for RHEED image interpretation [15–19]. Inspired by these pioneering works, we propose to use a deep learning (DL) approach for classification of oxidized and deoxidized substrates via their RHEED patterns, to resolve the above described problems. As mentioned above, due to the sample rotation, the RHEED signal can confidently indicate deoxidation only during short moments, when the electron beam is aligned with a lattice direction of the crystal. In contrast to recent propositions to use DL with RHEED for surface reconstruction identification [18, 19], we therefore propose a model which analyzes *sequences* of RHEED patterns (i.e. videos), instead of single images. To this end, we propose a two-stage deep learning model: The first stage is an autoencoder, which compresses each full-resolution RHEED image into a low-dimensional latent vector. The second stage subsequently determines the oxidation state for a sequence of such latent vectors, hence for the compressed representation of a short RHEED video sequence. We provide a detailed analysis of the required latent and sequence lengths and demonstrate the accuracy of the model as well as its stability over a period of more than 6 months between training data sampling and testing.

* e-mail : pwiecha@laas.fr

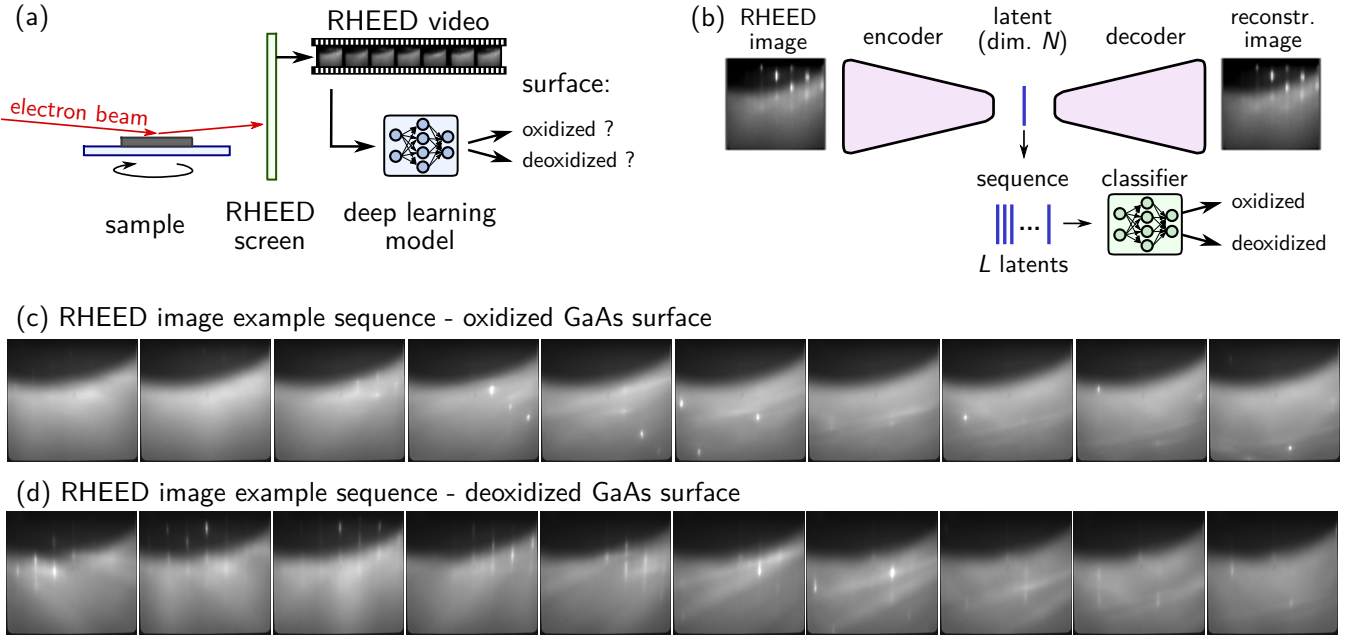


Figure 1. Deoxidation detection problem. (a) Short sequences of the RHEED video obtained from a rotating GaAs substrate are analyzed by a deep learning neural network model (NN), to determine if the substrate deoxidation process has terminated. (b) The DL model consists of two stages. An autoencoder encodes every single RHEED image into a latent vector of dimension N with the goal of reconstructing the original image. The latent thus contains all relevant features of the RHEED image. Sequences of L latent vectors are then used for classification of deoxidized surfaces. The classifier network thus analyses short RHEED videos covering a certain rotation angle. (c) Example sequence of 10 consecutive raw RHEED images obtained from an oxidized GaAs surface. (d) Example sequence of 10 consecutive raw RHEED images obtained after deoxidation from the same GaAs surface as shown in (c).

II. RESULTS AND DISCUSSION

A. Substrate deoxidation classification Problem

The general problem is schematically depicted in Figure 1a. Our goal is to precisely determine the moment of full oxyde removal from a GaAs substrate by monitoring the RHEED pattern during the deoxidation process. By feeding short video sequences of several consecutive RHEED images to a classification neural network, we aim at determining the oxidation state of the substrate surface, in order to reduce the necessity of human supervision of the substrate cleaning process. Visually, deoxidized surfaces are relatively easy to identify in the RHEED sequences due to the appearance of diffraction points (c.f. figure 1c-d), however, the patterns are not always visible due to the rotation of the sample and bright spots of less order can occur also from oxidized surfaces. Therefore an algorithmic classification is not entirely trivial.

B. Dataset

To train a neural network on deoxidation reconnaissance, we generate a training dataset by capturing RHEED videos before and after the oxide removal procedure. The images are collected in real time at 24 frames per second, while the sample rotates with 12 rounds per minute, hence we capture

120 images per full rotation. The RHEED video is thereby captured image by image, using a CMOS Camera (Allied Vision Manta G319B) with 4×4 pixel binning, resulting in raw images of 416×444 pixels at 12 bit grayscale intensity resolution. Those images are simply converted to 8 bit format and scaled to 100×100 pixels. In total we collected videos containing a total of 7644 RHEED images from five substrate oxide removal procedures within a period of a few days. 3110 of these images correspond to deoxidized surfaces, the rest are images from GaAs surfaces which were covered by a native oxide layer. We use 20% of the dataset for validation and the remaining 80% for training. In addition to the oxidized and deoxidized image sets, we also captured images during the full deoxidation procedure. These are not used during training and serve for testing of the algorithm. RHEED images during a further deoxidation were captured around 6 months after generation of the initial dataset. These serve for an assessment of the long-term stability of the classification.

C. RHEED sequence classifier network model

Our deoxidation monitor deep learning model is composed of two stages, as depicted schematically in figure 1b. A first stage is a feature extractor network, compressing the large RHEED images into compact latent vectors. This is done separately image by image. The second stage is the actual classification network. Its input are sequences of latent vectors,

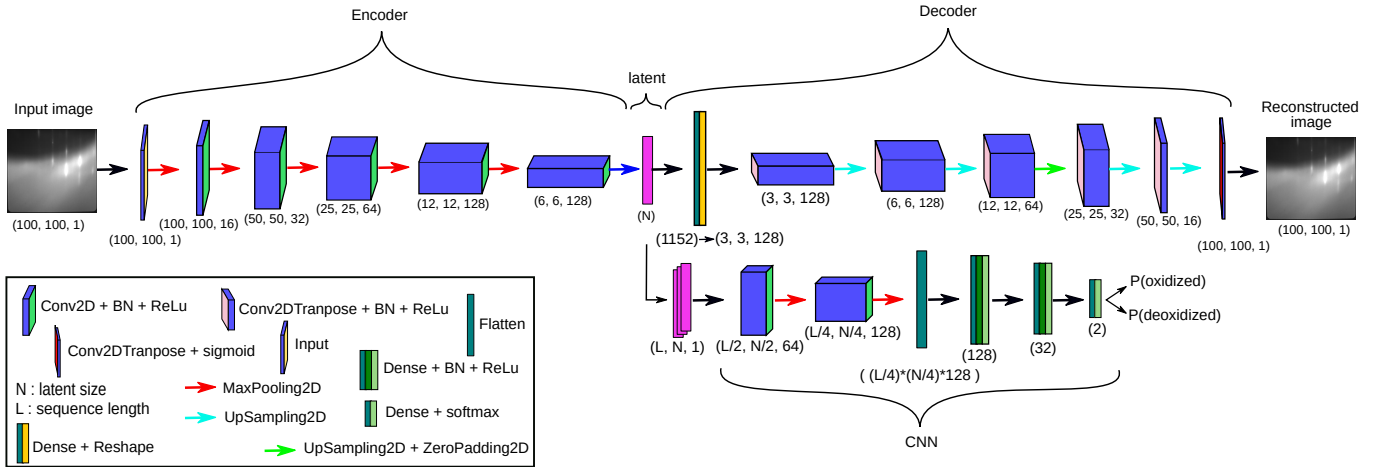


Figure 2. Detailed network architecture. In a CNN autoencoder (AE, top), each RHEED image is first compressed through a convolutional encoder into a 1D latent vector of length N . Training target of the AE is reconstruction of the original image from the latent vector (through the decoder stage, only used during training). The second stage of the model is a classifier CNN network (bottom right), taking as input a sequence of L latent vectors, corresponding to a series of RHEED images. These L latent vectors are stacked and passed into a CNN for classification into two classes: oxidized and deoxidized. All convolutions are followed by batch normalization (BN) [20] and ReLU activation. For descriptions of the different network layers we refer the interested reader to relevant literature [21].

corresponding to short RHEED videos.

1. *Image feature extraction*

As feature extractor we use a deep convolutional autoencoder neural network (AE), which has been reported to offer slightly superior compression quality compared to other dimensionality reduction methods such as principal component analysis (PCA), especially at high compression rates. We note however, that AEs require in general more computational resources. Thus, if computation speed is crucial, PCA could be used instead, for with only a moderate reduction in encoding performance is expected [22].

The model details of our AE are shown in the top row of figure 2. A RHEED image goes through the encoder stage, being compressed into a latent vector of dimensionality N . For training, the latent vector is fed into a decoder stage, which is an exact mirror of the encoder, except for replacing convolution layers by transpose convolutions and applying zero padding if required, to maintain correct image dimension. Through non-supervised training, the autoencoder learns to reconstruct the unlabeled input images from their learned latent vector representation.

Please note that we optimized the network for low parameter number, in order to have a computationally efficient model. To this end we do not double the number of channels once a depth of 128 filters is reached. We also compared the architecture with a ResNet [23, 24], replacing the single convolutions by residual convolutional blocks each of which employing a sequence of 3 convolutions. The performance is similar and offers no advantage in deoxidation classification. Please note that this applies to the specific here discussed problem, for other problems the slightly improved accuracy offered by a

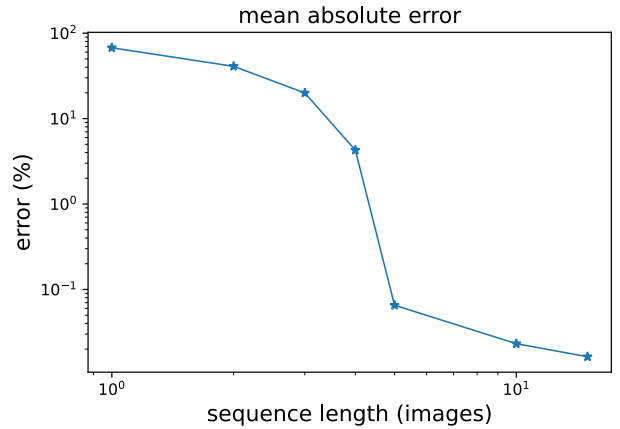


Figure 3. Prediction fidelity vs. sequence length. Mean absolute error on the test-set for network models working with increasing sequence length. The latent size is fixed to $N = 50$. The actual classification error of sequences $L \geq 5$ is zero.

ResNet may very well be beneficial.

2. Sequence classification CNN

The second stage of our model is the actual classification network. Because the MBE sample is rotating, the RHEED images are constantly varying. Especially during deoxidation, the surface is not atomically flat and signatures of oxide removal often occur in the RHEED images only when the electron beam is aligned with the crystal lattice of the substrate. For a high accuracy we therefore classify *sequences* of RHEED images, i.e. short videos. To do so, we compress the

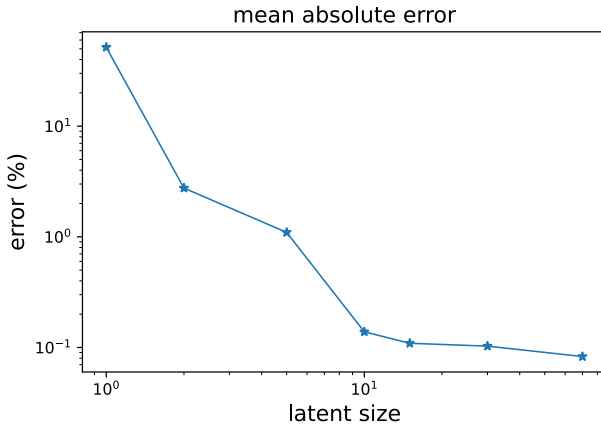


Figure 4. **Prediction fidelity vs. latent dimension.** Mean absolute error on the test-set for network models working with increasing latent dimension. The used sequence length is $L = 15$. The actual classification error with latent size $N \geq 10$ is virtually zero.

RHEED video image by image using the trained AE. Using the results we then create sequences of L consecutive latent vectors. These sequences are arranged as 2D arrays of size (L, N) , and are fed into a 2D convolutional classifier network with two output classes, one for oxidized and the second for deoxidized state of the surface. The details of the network are shown in the bottom right of figure 2. It is trained in a supervised manner of the dataset, with the goal to predict the correct surface state from a sequence of compressed RHEED images

D. Results

1. Autoencoder reconstruction quality

For the tuning of the autoencoder architecture we qualitatively tested AE layouts with varying number of layers and convolutional kernels by compressing and reconstructing random RHEED images that were not used for training. Once a layout was found that accurately reproduced the visual appearance of our RHEED images, we tested the reconstruction quality via peak signal to noise ratio (PSNR), where the original image is used as the signal and the difference between original and reconstructed image as noise. We obtained the best PSNR for $N = 70$ with a value of around 90, no further improvement was observed for larger latent dimensions.

2. Classification accuracy

We test the classification accuracy of the full two-stage model (AE + classifier) with different values for the sequence length and fixed latent size $N = 50$, as well as for varying latent dimensions while fixing the sequence length $L = 15$. We find that the sequence length L is indeed a crucial parameter. Single-image classification basically fails. Sequences of

at least $L = 5$ images are required, to drop the error rates well below 1%, which can be seen in figure 3. Concerning the latent size, we require at least a compression dimensionality of $N = 10$ in order to get error rates well below 1%, increasing latent dimension further improves the accuracy only marginally. This is shown in figure 4.

Subsequently we test whether the network is capable to determine the exact moment of deoxidation on a set of images captured during the entire deoxidation procedure. First we fix the latent size to $N = 50$ and increase the sequence length successively from $L = 1$ to $L = 15$ (figure 5 top row). In agreement with the former test (figure 3), we find that starting from sequence lengths of $L = 5$ the network works accurately and essentially error-free. It detects the precise moment of deoxidation with an agreement of a few seconds compared to the estimation of the human operator. We then fix the sequence length to $L = 15$ and vary the latent dimension between $N = 1$ and $N = 70$ (figure 5 bottom row). For latent vectors of dimension $N = 10$ or larger, we find again quasi error-free classification and precise determination of the deoxidation moment.

We conclude that the smallest data size for accurate operation is a latent dimension of $N = 10$ and a sequence length of $L = 5$. At a video rate of 120 images per full rotation of the substrate holder, this sequence length ($L = 5$) corresponds to a rotation angle of 15 degrees being concurrently processed by the classifier network.

3. Temporal stability of the classification accuracy

An MBE is a highly complex apparatus, housing many parts that have a potential impact on the long-term stability of the RHEED precision. To name a few, multiple pumps are required to maintain an ultra-high vacuum, hot source chambers are distributed around the chamber, and mechanical stress is applied to the sample holder. It is not only constantly rotating but also repeatedly heated up and cooled down by temperature differences of many hundred degrees Kelvin. In addition to all these mechanical perturbations, it is very hard to avoid deposition of source material on the RHEED screen, slowly altering the RHEED images during an epitaxy campaign. In consequence, a constant RHEED image quality can usually not be guaranteed on a long-term. Deep learning being a data-based technique, a main advantage is generally a high robustness against noise and perturbations, provided that the training data is sufficiently rich [25]. We therefore expect our approach to deliver reliable classification results over significant time periods.

In order to assess whether our approach can provide accurate deoxidation detection over durations of typical crystal growth campaigns, we recorded a deoxidation RHEED video around 6 months after the acquisition of the training data. Its classification results are shown in figure 6. While we observe a slightly reduced classification certainty regarding the exact moment of deoxidation, even 6 months after initial training data recording, the non-retrained neural network still performs sufficiently well on the deoxidation detection. We want to note that after a few additional training epochs on a small set

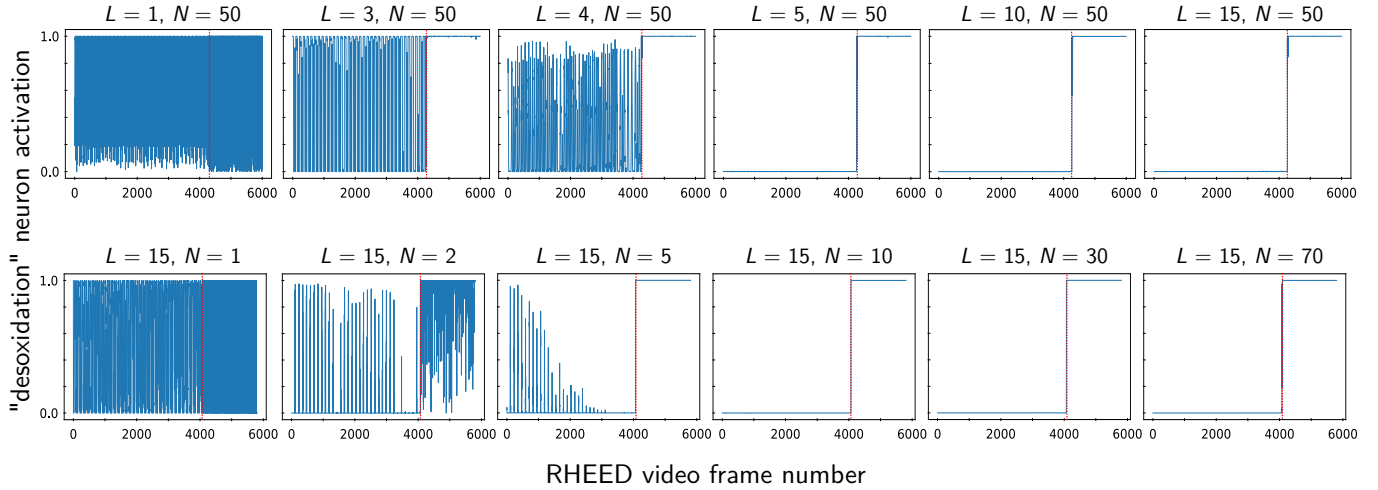


Figure 5. Detection accuracy of deoxidation moment. The impact of the sequence length as well as of latent vector dimension is tested on a video captured during a full deoxidation. The video consists of 31,819 RHEED images, of which the last 6,000 are shown. Deoxidation occurs around 1,800 frames before the sequence end (indicated by a red dotted line). The RHEED video is captured with 24 frames per second. Top row: Increasing sequence length L , the latent dimension of the autoencoder is fixed to $N = 50$. Bottom row: Increasing latent dimension N , the sequence length of the classifier is fixed to $L = 15$.

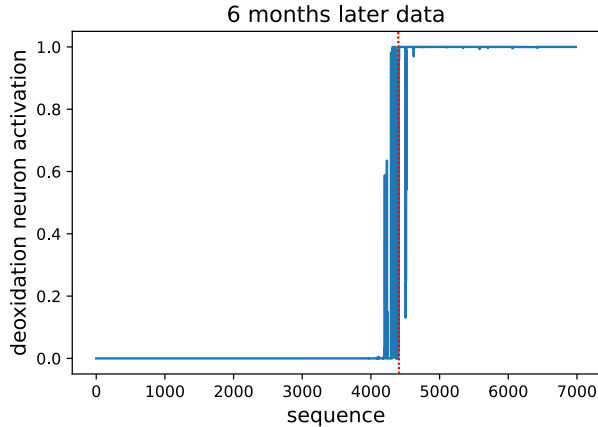


Figure 6. Test on six month newer data. Evaluation of a deoxidation RHEED video recorded 6 months after the training data, using the network model with latent dimension $N = 50$ and a sequence length $L = 15$. The network model was not re-trained.

of new images, the fidelity of the network reaches the same confidence as observed in the right-hand panels of figure 5.

III. CONCLUSIONS

In conclusion we presented a deep learning model based on a 2D convolutional neural network to detect the surface

oxidation state of GaAs substrates from raw RHEED image sequences, as typically available in molecular beam epitaxy. Our model consists of a first autoencoder neural network, which learns to compress individual RHEED images to a low-dimensional latent space. Sequences of consecutive, compressed RHEED images are then classified for their surface oxidation state through a second convolutional network. We presented a systematic analysis of classification performance as function of used compression ratio as well as RHEED video sequence length. We demonstrated that the model accurately identifies the exact surface deoxidation moment and that the performance is robust during at least 6 months of MBE operation without requiring re-training. Our approach is very appealing thanks to its simplicity and low computational cost. Without requiring additional hardware it can hence be easily set up in any RHEED equipped MBE.

ACKNOWLEDGMENTS

This work was supported by the Toulouse HPC CALMIP (grant p20010). This study benefited from the support of both the LAAS-CNRS micro and nanotechnologies platform, member of the French RENATECH network, and the EPI-CENTRE common laboratory between Riber and CNRS.

[1] Ino, S. Some New Techniques in Reflection High Energy Electron Diffraction (RHEED) Application to Surface Structure

Studies. *Japanese Journal of Applied Physics* **16**, 891 (1977).

[2] Horio, Y., Hashimoto, Y. & Ichimiya, A. A new type of RHEED apparatus equipped with an energy filter. *Applied Surface Science* **100–101**, 292–296 (1996).

[3] Braun, W. *Applied RHEED: Reflection High-Energy Electron Diffraction during Crystal Growth*. Springer Tracts in Modern Physics (Springer Berlin Heidelberg, 1999).

[4] Ichimiya, A., Cohen, P. & Cohen, P. *Reflection High-Energy Electron Diffraction* (Cambridge University Press, 2004).

[5] of Surfaces, N. A. S. I. o. t. S., Techniques, I. b. E. O., Valdre, U. & Howie, A. *Surface and Interface Characterization by Electron Optical Methods / Edited by A. Howie and U. Valdre* (Plenum Press : Published in cooperation with the NATO Scientific Affairs Division New York, 1988).

[6] Jo, J., Tchoe, Y., Yi, G.-C. & Kim, M. Real-Time Characterization Using *in situ* RHEED Transmission Mode and TEM for Investigation of the Growth Behaviour of Nanomaterials. *Scientific Reports* **8**, 1694 (2018).

[7] Thelander, C., Caroff, P., Plissard, S. & Dick, K. A. Electrical properties of InAs_{1-x}S_x and InSb nanowires grown by molecular beam epitaxy. *Applied Physics Letters* **100**, 232105 (2012).

[8] Daudin, B. *et al.* How to grow cubic GaN with low hexagonal phase content on (001) SiC by molecular beam epitaxy. *Journal of Applied Physics* **84**, 2295–2300 (1998).

[9] Ohtake, A., Mano, T. & Sakuma, Y. Strain relaxation in InAs heteroepitaxy on lattice-mismatched substrates. *Scientific Reports* **10**, 4606 (2020).

[10] Sacha, G. M. & Varona, P. Artificial intelligence in nanotechnology. *Nanotechnology* **24**, 452002 (2013).

[11] Ren, J.-C., Liu, D. & Wan, Y. Modeling and application of Czochralski silicon single crystal growth process using hybrid model of data-driven and mechanism-based methodologies. *Journal of Process Control* **104**, 74–85 (2021).

[12] Schimmel, S., Sun, W. & Dropka, N. Artificial Intelligence for Crystal Growth and Characterization. *Crystals* **12**, 1232 (2022).

[13] Choudhary, K. *et al.* Recent advances and applications of deep learning methods in materials science. *npj Computational Materials* **8**, 1–26 (2022).

[14] Battie, A. Y., Valero, A. C., Horwat, D. & Naciri, A. E. Rapid ellipsometric determination and mapping of alloy stoichiometry with a neural network. *Optics Letters* **47**, 2117–2120 (2022).

[15] Brown, T. *et al.* Modeling MBE RHEED signals using PCA and neural networks. In *Compound Semiconductors 1997. Proceedings of the IEEE Twenty-Fourth International Symposium on Compound Semiconductors*, 33–36 (1997).

[16] Vasudevan, R. K., Tselev, A., Baddorf, A. P. & Kalinin, S. V. Big-Data Reflection High Energy Electron Diffraction Analysis for Understanding Epitaxial Film Growth Processes. *ACS Nano* **8**, 10899–10908 (2014).

[17] Provence, S. R. *et al.* Machine Learning Analysis of Perovskite Oxides Grown by Molecular Beam Epitaxy. *Physical Review Materials* **4**, 083807 (2020). 2004.00080.

[18] Kwoen, J. & Arakawa, Y. Classification of Reflection High-Energy Electron Diffraction Pattern Using Machine Learning. *Crystal Growth & Design* **20**, 5289–5293 (2020).

[19] Kwoen, J. & Arakawa, Y. Multiclass classification of reflection high-energy electron diffraction patterns using deep learning. *Journal of Crystal Growth* **593**, 126780 (2022).

[20] Ioffe, S. & Szegedy, C. Batch Normalization: Accelerating Deep Network Training by Reducing Internal Covariate Shift. *arXiv:1502.03167 [cs]* (2015). 1502.03167.

[21] Goodfellow, I., Bengio, Y. & Courville, A. *Deep Learning* (MIT Press, 2016).

[22] Fournier, Q. & Aloise, D. Empirical Comparison between Autoencoders and Traditional Dimensionality Reduction Methods. In *2019 IEEE Second International Conference on Artificial Intelligence and Knowledge Engineering (AIKE)*, 211–214 (2019).

[23] He, K., Zhang, X., Ren, S. & Sun, J. Deep Residual Learning for Image Recognition. *arXiv:1512.03385 [cs]* (2015). 1512.03385.

[24] Szegedy, C., Ioffe, S., Vanhoucke, V. & Alemi, A. Inception-v4, Inception-ResNet and the Impact of Residual Connections on Learning. In *Proceedings of the Thirty-First AAAI Conference on Artificial Intelligence*, 4278–4284 (2016). 1602.07261.

[25] Kürüm, U., Wiecha, P. R., French, R. & Muskens, O. L. Deep learning enabled real time speckle recognition and hyperspectral imaging using a multimode fiber array. *Optics Express* **27**, 20965–20979 (2019).